

MITIGATION OF BEAM INSTABILITIES IN THE ECHO-ENABLED HARMONIC GENERATION BEAMLINE FOR FLASH2020+

F. Pannek*, W. Hillert, D. Samoilenko, University of Hamburg, Hamburg, Germany
S. Ackermann, E. Allaria, P. Niknejadi, G. Paraskaki, L. Schaper
Deutsches Elektronen-Synchrotron DESY, Hamburg, Germany
M. Pop, MAX IV Laboratory, Lund, Sweden

Abstract

With the FLASH2020+ upgrade, one of the beamlines of the free-electron laser FLASH at DESY will be based on the Echo-Enabled Harmonic Generation (EEHG) seeding scheme and provide high-repetition-rate, coherent radiation down to 4 nm. To reach this wavelength, it is necessary to imprint intricate structures on the longitudinal phase space of the electron bunch at a very high harmonic of the seed laser wavelength, making the scheme potentially vulnerable to beam instabilities. Part of the beamline is a strong chicane, which is necessary to create the dispersion required by EEHG. Resulting effects such as Coherent Synchrotron Radiation (CSR) can be very detrimental for the bunching process and have to be taken into account already in the design of the beamline to ensure optimum FEL performance. We investigate and propose possible mitigation solutions to such instabilities in the FLASH2020+ parameter range.

INTRODUCTION

In the course of the FLASH2020+ upgrade [1] of the superconducting free-electron laser (FEL) user facility FLASH [2–4] in Hamburg, Germany, it is foreseen that one of the beamlines will be based on the Echo-Enabled Harmonic Generation (EEHG) seeding scheme [5]. EEHG provides a defined electron beam density distribution, which makes the startup process in the FEL not dependent on the stochastic nature of the shot noise and thus allows for shot-to-shot reproducibility of fourier limited pulses [6, 7]. However, beam instabilities arising within the EEHG section could be a limiting factor to achieve the necessary bunching [8]. Intrabeam Scattering (IBS) and Incoherent Synchrotron Radiation (ISR) have been studied based on analytical formulas [9] for the FLASH2020+ parameter space and result in no significant reduction of the bunching.

Coherent Synchrotron Radiation (CSR) describes the phenomenon that electrons traveling through a dipole magnet can emit coherent radiation at wavelengths comparable to the bunch length. Due to the curved trajectory, the radiation can take a shortcut, which leads to a tail-head interaction. This finally results in an energy modulation along the bunch [10]. In the following, the effect of this energy modulation on the bunching is studied with the general-purpose accelerator simulation code ELEGANT [11] for EEHG at 4 nm. Two mitigation solutions, taking into account the duration of the seed laser and different EEHG working points, are examined.

* fabian.pannek@desy.de

THEORY

In the EEHG seeding scheme, the longitudinal phase space distribution of the electron bunch is manipulated in a beamline which consists of two undulators, so-called modulators, and two chicanes, as shown in Fig. 1.

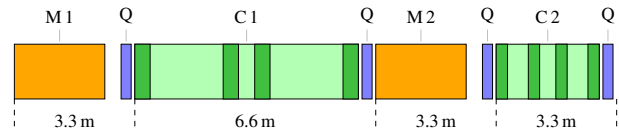


Figure 1: EEHG beamline used in the simulations with Modulators (M), Quadrupoles (Q) and Chicanes (C).

In each modulator the electron bunch is modulated in energy by interacting with a seed laser, described by the energy modulation amplitudes $A_{1,2} = \Delta E_{1,2}/\sigma_E$, that is the energy modulation ΔE produced by the seed laser expressed as a multiple of the beam energy spread σ_E . The first chicane is used to create multiple energy bands in the longitudinal phase space and therefore requires a large dispersion $R_{56}^{(1)}$. The second dispersive section, described by $R_{56}^{(2)}$, compresses the energy modulated bands, creating a density modulation at the wavelength $\lambda_E = \lambda_1/a_E$. For two seed lasers operating at the same wavelength $\lambda_1 = \lambda_2$, the harmonic number is given by $a_E = n + m$, where n and m are non-zero integers of opposite signs. The degree of bunching is described by the bunching factor $|b_{n,m}|$. Its maximum value is approached for $A_1 \gtrsim 3$ and $n = -1$ and it scales approximately as $|b_{-1,m}| \approx 0.39 \cdot m^{-1/3}$ for $m > 4$ [12]. For optimized bunching at a specific harmonic, the ratio of the dispersions has to be close to $R_{56}^{(1)}/R_{56}^{(2)} \approx a_E/|n|$. Since the required strength of the second chicane is inversely proportional to the energy modulation imposed in the second modulator, $R_{56}^{(2)} \propto 1/A_2$, a large A_2 decreases the required dispersion of both chicanes. This is, however, accompanied by an increase in energy spread, resulting in a decreased FEL performance.

CSR STUDY

For this study, a $\sigma_z = 100 \mu\text{m}$ Gaussian electron beam with an energy of $E = 1.35 \text{ GeV}$, an energy spread of $\sigma_E = 150 \text{ keV}$, a peak current of $I_p = 500 \text{ A}$ and a normalized emittance of $\varepsilon_n = 0.6 \text{ mm mrad}$ is used. Both seed lasers are set to $\lambda_{1,2} = 300 \text{ nm}$. The chicane and modulator parameters used for the simulations are shown in Table 1. Each modulator and chicane is followed by quadrupoles to

ensure proper matching. The energy modulation amplitudes are set to $A_1 = 3$ and $A_2 = 5$. The corresponding bunching factor $|b|$ can be calculated analytically and is shown in Fig. 2 for different chicane configurations. Since maximum bunching can be achieved for $n = -1$, simulations with the FEL code GENESIS1.3, v4 [13, 14] have been carried out for this case to optimize the dispersive strengths for power gain and spectral properties in the radiator beamline. For the upper bunching peak in Fig. 2 optimum values were found to be $R_{56}^{(1)} = 7.05$ mm and $R_{56}^{(2)} = 81.25$ μ m.

Table 1: Simulation Beamline Parameters

| Chicanes | 1 | 2 | Modulators | |
|-------------------------|-------|-------|------------------|------|
| length (m) | 6.124 | 2.824 | λ_u (mm) | 82.6 |
| L_{dipole} (m) | 0.42 | 0.31 | Periods | 30 |
| L_{drift} (m) | 2.00 | 0.57 | K | 9.97 |

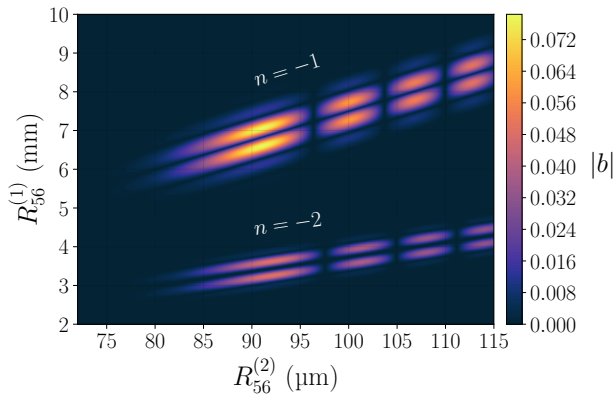


Figure 2: Bunching factor of the 75th harmonic of 300 nm as a function of different dispersive strengths of the first and second chicane for $A_1 = 3$ and $A_2 = 5$.

Method

The working point is adopted to ELEGANT, which makes use of an 1D CSR model to calculate the energy change of a line-charge distribution in a dipole magnet [10, 15]. The propagation of the CSR wake through drift spaces and subsequent elements is also taken into account. For this study, an infinite duration of the two seed lasers is used to monitor the bunching along the whole electron bunch.

To calculate the bunching, the electron bunch is subdivided into slices of length L_{slice} . Within a slice, a phase ϕ_k is assigned to each of the n particles, according to

$$\phi_k = \frac{s_k - s_0}{L_{\text{slice}}} \cdot 2\pi, \quad (1)$$

with s_k being the longitudinal coordinate of the particle and s_0 being the beginning of the slice. The bunching at a specific wavelength λ_0 is then calculated by

$$|b| = \left| \frac{1}{n} \sum_{k=1}^n \exp\left(-i\phi_k \frac{L_{\text{slice}}}{\lambda_0}\right) \right|. \quad (2)$$

The bunching is determined at the end of the EEHG section.

Duration of the Second Seed Laser

The induced energy modulation along the bunch due to CSR in the first chicane can be seen in the top plot of Fig. 3. While calculating the bunching of the whole electron bunch at the end of the beamline, the bunching is reduced from 5.9% to 1.3% when incorporating CSR effects.

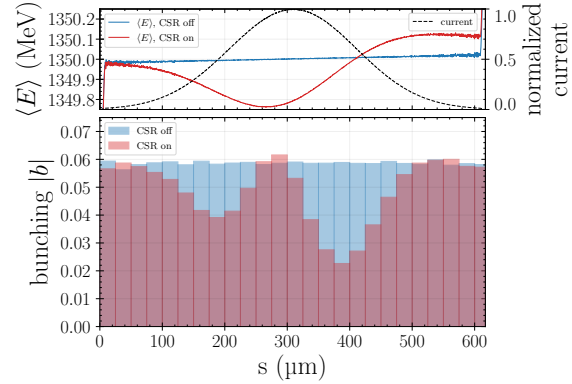


Figure 3: *Top*: Energy averaged over 300 nm along the bunch without and with incorporated CSR before entering the second modulator together with the current profile. *Bottom*: Bunching factor at 4.0 nm calculated within slices of 25 μ m length along the bunch without and with incorporated CSR.

To investigate the effect of a second seed laser with a pulse duration much shorter than the bunch, the slice length within the bunching is calculated is set to $L_{\text{slice}} = 25$ μ m, which corresponds to approximately $4\sigma_z$ of the second seed laser ($\sigma_z \approx 6.37$ μ m) that will be used for FLASH2020+. The bottom plot of Fig. 3 shows that the bunching at $\lambda_E = 4.0$ nm is reduced the most in areas where the CSR induced change in energy is large. However, there exists also a region near the center of the bunch with no reduction in bunching.

To better investigate the phenomenon associated to the bunching reduction, the bunching is calculated not only at the exact seed laser harmonic λ_E but also at wavelengths close to it. By using Eq. (2) for different wavelengths one can reconstruct the spectral content of the bunching produced by the seed at different positions along the bunch, as shown in Fig. 4. The data show that the bunching reduction reported in Fig. 3 corresponds to a wavelength shift of the bunching. This suggests that for a case with a short seed the overall

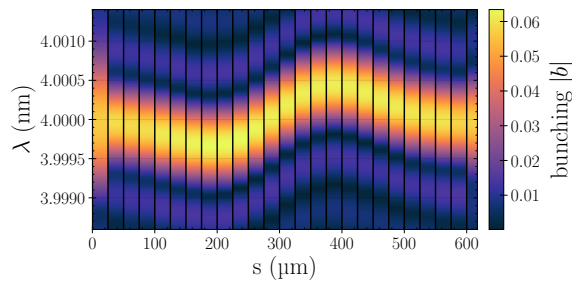


Figure 4: Bunching factor at different wavelengths calculated within slices of 25 μ m length along the bunch with CSR.

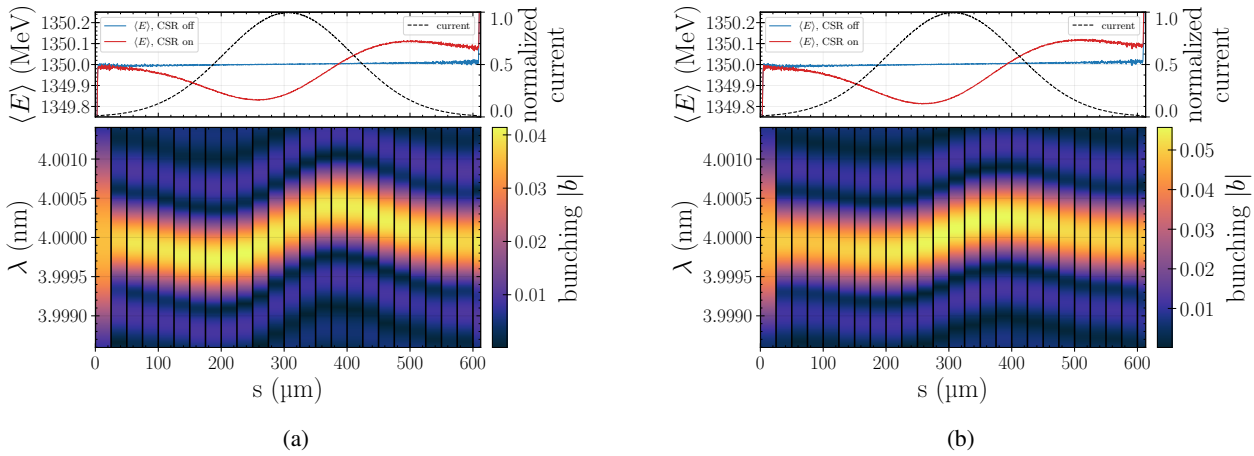


Figure 5: (a) $n = -2$ working point for $A_2 = 5$ to reduce the dispersion of the first chicane. (b) $n = -1$ working point for $A_2 = 8$ to reduce the dispersion of both the first and the second chicane. *Top*: Energy averaged over 300 nm along the bunch without and with incorporated CSR before entering the second modulator together with the current profile. *Bottom*: Bunching factor at different wavelengths calculated within slices of $25 \mu\text{m}$ length along the bunch with CSR incorporated.

bunching will not be reduced, but the emission wavelength will depend on the timing between the electron beam and the seed laser and wavelength fluctuations may arise as a result of the timing jitter. Even though it is expected that the jitter will be well within the duration of the shown slices, it would be possible to seed at areas of the bunch with a linear change in energy to diminish this wavelength dependency.

Different Working Points

Another possibility to mitigate the detrimental effect of CSR on bunching is to change the EEHG working point. The required $R_{56}^{(1)}$ of the first chicane reduces by a factor of about 2 when switching to the $n = -2$ configuration. Based on GENESIS1.3 simulations, the dispersion strengths were set to $R_{56}^{(1)} = 3.27 \text{ mm}$ and $R_{56}^{(2)} = 82.75 \mu\text{m}$, corresponding to the lower bunching peak in Fig. 2. Consequently the dipoles of the chicane have to be less strong and the induced energy modulation due to CSR is less prominent, as can be seen in Fig. 5a. Concerning the bunching, there is no significant improvement and because of the overall smaller bunching the $n = -2$ working point is not a preferable option.

To explore a working point with a reduced dispersive strength of both the first and second chicane, the energy modulation amplitude is increased to $A_2 = 8$. Here too, an optimum chicane setup was determined by means of GENESIS1.3 simulations, aiming for the lower $n = -1$ bunching peak in Fig. 6. The resulting dispersive strengths are $R_{56}^{(1)} = 4.033 \text{ mm}$ and $R_{56}^{(2)} = 47.25 \mu\text{m}$. As expected, Fig. 5b shows that the induced energy modulation is now slightly more pronounced compared to the previous $n = -2$ case, because of the larger $R_{56}^{(1)}$. However, there is a clear improvement concerning wavelength shift of the bunching, making it possible to also seed larger parts of the bunch without a significant reduction in bunching. This is a consequence of the smaller dispersion of the second chicane, which translates the energy slope arising in the first chicane into a wavelength shift in bunching [16, 17].

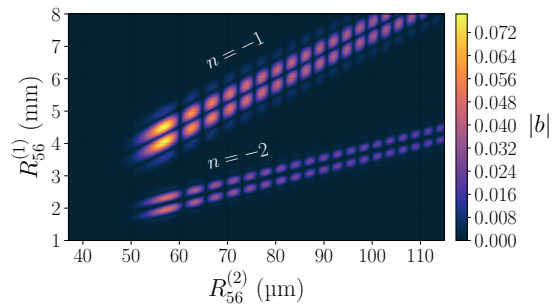


Figure 6: Bunching factor of the 75th harmonic of 300 nm as a function of different dispersive strengths of the first and second chicane for $A_1 = 3$ and $A_2 = 8$.

CONCLUSION

In the first chicane CSR induces an energy modulation along the bunch, which finally results in a wavelength shift of the bunching, depending on the position in the bunch. The deterioration of the bunching can either be mitigated by seeding only a small part of the bunch by using a short second seed laser, as it will be the case for FLASH2020+. Another possibility is to utilize another EEHG working point to reduce the required dispersion of the second chicane. This can be achieved by increasing the energy modulation amplitude in the second modulator, which is, however, accompanied by an increase in energy spread.

ACKNOWLEDGEMENTS

This research was supported through the Maxwell computational resources operated at DESY, Hamburg. This work has been financially supported by BMBF within the project "05K2019-STAR". The authors acknowledge the funding through the Lund-Hamburg 'IFELD' collaboration. G. P. would like to thank Helmholtz InterLabs-0002 CHILFEL for financial support.

REFERENCES

- [1] E. Allaria *et al.*, “FLASH2020+ plans for a new coherent source at DESY”, presented at the 12th Int. Particle Accelerator Conf. (IPAC’21), Campinas, Brazil, 2021, paper TU-PAB086, this conference.
- [2] W. Ackermann *et al.*, “Operation of a free-electron laser from the extreme ultraviolet to the water window”, *Nature Photonics*, vol. 1, pp. 336-342, 2007. doi:10.1038/nphoton.2007.76
- [3] S. Schreiber and B. Faatz, “The free-electron laser FLASH”, *High Power Laser Science and Engineering*, vol. 3, p. E20, 2015. doi:10.1017/hpl.2015.16
- [4] B. Faatz *et al.*, “Simultaneous operation of two soft x-ray free-electron lasers driven by one linear accelerator”, *New Journal of Physics*, vol. 18, p. 062002, 2016. doi:10.1088/1367-2630/18/6/062002
- [5] G. Stupakov, “Using the Beam-Echo Effect for Generation of Short-Wavelength Radiation”, *Physical Review Letters*, vol. 102, p. 074801, 2009. doi:10.1103/PhysRevLett.102.074801
- [6] E. Hemsing, G. Stupakov, D. Xiang, and A. Zholents, “Beam by design: Laser manipulation of electrons in modern accelerators”, *Reviews of Modern Physics*, vol. 86, pp. 897-941, 2014. doi:10.1103/RevModPhys.86.897
- [7] G. Penn, “Stable, coherent free-electron laser pulses using echo-enabled harmonic generation”, *Physical Review Special Topics - Accelerators and Beams*, vol. 17, p. 110707, 2014. doi:10.1103/PhysRevSTAB.17.110707
- [8] E. Hemsing, “Bunching phase and constraints on echo enabled harmonic generation”, *Physical Review Accelerators and Beams*, vol. 21, p. 050702, 2018. doi:10.1103/PhysRevAccelBeams.21.050702
- [9] G. Penn, “EEHG Performance and Scaling Laws”, LBNL, Berkeley, CA, USA, Rep. LBNL-6481E, 2013. doi:10.2172/1164809
- [10] E. L. Saldin, E. A. Schneidmiller, and M. V. Yurkov, “On the coherent radiation of an electron bunch moving in an arc of a circle”, *Nuclear Instruments and Methods in Physics Research Section A: Accelerators, Spectrometers, Detectors and Associated Equipment*, vol. 398, pp. 373-394, 1997. doi:10.1016/S0168-9002(97)00822-X
- [11] M. Borland, “ELEGANT: A Flexible SDDS-Compliant Code for Accelerator Simulation”, Argonne National Lab., Argonne, IL, USA, Rep. LS-287, Aug. 2000. doi:10.2172/761286
- [12] D. Xiang and G. Stupakov, “Echo-enabled harmonic generation free electron laser”, *Physical Review Special Topics - Accelerators and Beams*, vol. 12, p. 030702, 2009. doi:10.1103/PhysRevSTAB.12.030702
- [13] S. Reiche, “GENESIS 1.3: a fully 3D time-dependent FEL simulation code”, *Nuclear Instruments and Methods in Physics Research Section A: Accelerators, Spectrometers, Detectors and Associated Equipment*, vol. 429, pp. 243-248, 1999. doi:10.1016/S0168-9002(99)00114-X
- [14] S. Reiche, “Update on the FEL Code Genesis 1.3”, in *Proc. 36th Int. Free Electron Laser Conf. (FEL’14)*, Basel, Switzerland, Aug. 2014, paper TUP019, pp. 403-407.
- [15] M. Borland, “Simple method for particle tracking with coherent synchrotron radiation”, *Physical Review Special Topics - Accelerators and Beams*, vol. 4, p. 070701, 2001. doi:10.1103/PhysRevSTAB.4.070701
- [16] Z. Huang, D. F. Ratner, G. V. Stupakov, and D. Xiang, “Effects of Energy Chirp on Echo-enabled Harmonic Generation Free Electron Lasers”, in *Proc. 31st Int. Free Electron Laser Conf. (FEL’09)*, Liverpool, UK, Aug. 2009, paper MOPC45, pp. 127-129.
- [17] Z. Zhao *et al.*, “First lasing of an echo-enabled harmonic generation free-electron laser”, *Nature Photonics*, vol. 6, pp. 360-363, 2012. doi:10.1038/nphoton.2012.105